

Transverse instability and magnetic structures associated with electron phase space holes

Aimin Du,¹ Mingyu Wu,² Quanming Lu,^{2,a)} Can Huang,² and Shui Wang²

¹*Institute of Geology and Geophysics, Chinese Academy of Sciences, Beijing 100029, China*

²*CAS Key Laboratory of Basic Plasma Physics, School of Earth and Space Sciences, University of Science and Technology of China, Hefei, Anhui 230026, China*

(Received 10 December 2010; accepted 9 February 2011; published online 8 March 2011)

Electron phase space holes (electron holes) are found to be unstable to the transverse instability. Two-dimensional (2D) electromagnetic particle-in-cell simulations are performed to investigate the structures of the fluctuating magnetic field associated with electron holes. The combined actions between the transverse instability and the stabilization by the background magnetic field ($\mathbf{B}_0 = B_0 \hat{\mathbf{e}}_x$) lead a one-dimensional electron hole into several 2D electron holes which are isolated in both the x and y directions. The electrons trapped in these 2D electron holes suffer the electric field drift $\mathbf{v}_E = \mathbf{E} \times \mathbf{B}_0 / B_0^2$ due to the existence of the perpendicular electric field E_y , which generates the current along the z direction. Then, the unipolar and bipolar structures are formed for the parallel cut of the fluctuating magnetic field along the x and y directions, respectively. At the same time, these 2D electron holes move along the x direction, and the unipolar structures are formed for the parallel cut of the fluctuating magnetic field along the z direction. © 2011 American Institute of Physics. [doi:10.1063/1.3561796]

I. INTRODUCTION

Electron phase space holes (electron holes) are ubiquitously observed in space plasma, such as in the auroral region, the transition region of the bow shock, the solar wind, the magnetopause, and the magnetic sheath.^{1–6} Electron holes are considered to be the stationary BGK (Bernstein-Greene-Kruskal) solution of the Vlasov and Poisson equations, and they have positive potential pulses.^{7–9} Particle-in-cell (PIC) simulations have revealed that electron holes can be formed during the nonlinear evolution of electron bistream instabilities, which is consistent with the theoretical predictions.^{10–12}

The observational characteristics of electrostatic structures in electron holes have been reported in a number of articles. In electron holes, the parallel cut of the parallel electric field (E_{\parallel}) is found to have bipolar structures, while the parallel cut of the perpendicular electric field (E_{\perp}) has unipolar structures.^{13–15} Such structures have already been found in electron holes formed during the nonlinear evolution of multidimensional electron bistream instabilities.^{16–18} Recently, with the help of two-dimensional (2D) electrostatic PIC simulations, Lu *et al.*¹⁹ investigated the features of electron holes formed during the nonlinear evolution of electron bistream instabilities in magnetized plasma and found that such electrostatic structures of these electron holes are governed by the interactions between the transverse instability and the stabilization effects by the background magnetic field \mathbf{B}_0 . At the same time, the unipolar structures of the parallel cut of E_{\perp} as well as the bipolar structures of the parallel cut of E_{\parallel} can be formed in the electron holes. The transverse instability was proposed by Muschietti *et al.*,²⁰ and it is a

self-focusing type of instability due to the dynamics of the trapped electrons in electron holes. Perturbations in electron holes can produce transverse gradients of the electric potential. Such transverse gradients focus the trapped electrons into regions that already have a surplus of electrons, which leads to larger transverse gradients and more focusing. At last, the transverse instability occurs in these electron holes.

In this paper, by performing 2D self-consistent PIC simulations we investigate the interactions between the transverse instability and the stabilization by the magnetic field in electron holes, with emphasis on the structures of the fluctuating magnetic field. We demonstrate that regular structures of the fluctuating magnetic field can be formed in electron holes due to the transverse instability. Their three-dimensional (3D) structures are also discussed and compared with the observational characteristics of the fluctuating magnetic field in the electron holes, which was recently measured by the THEMIS mission.²¹

II. SIMULATION MODEL

A 2D (two spatial dimensions, all three velocity components) electromagnetic PIC code with periodic boundary conditions is employed in our simulations. The code retains the full dynamics of electrons, while ions form a neutralizing background. The electric and magnetic fields are defined on the grids and obtained by integrating the time dependent Maxwell equations with a full explicit algorithm.²² The background magnetic field \mathbf{B}_0 is along the x direction. Initially, a potential structure, which represents a one-dimensional (1D) electron hole, is located in the middle of the simulation domain. The 1D electron hole has limited extent in the x direction, while it is infinite in the y direction. The potential structure is described as²³

^{a)}Author to whom correspondence should be addressed. Electronic mail: qmlu@ustc.edu.cn

$$\phi(x) = \psi \exp[-0.5(x-L)^2/\Delta_{\parallel}^2], \quad (1)$$

where Δ_{\parallel} and L are the half width and the center position of the electron hole, respectively, and ψ is the amplitude of the potential structure. The potential structure, which is supported by a clump of trapped electrons, is homogeneous in the transverse direction. The trapped electrons gyrate in the background magnetic field, and simultaneously they bounce back and forth along the parallel direction in the electron hole. The motions of a trapped electron are determined by the ratio of the electron gyrofrequency $\Omega_e = eB_0/m_e$ to the bounce frequency $\omega_b = \sqrt{\psi/\Delta_{\parallel}^2}$.²⁰ The initial electron distributions can be calculated by the BGK method self-consistently, which has already been given by Muschietti *et al.*²³ It is

$$F(x, v_x, v_y, v_z) = F_1(w) \exp[-0.5(v_y^2 + v_z^2)/T_e], \quad (2)$$

where T_e is the electron temperature and $w \equiv v_x^2 - 2\phi(x)$ is twice the parallel energy. In addition,

$$F_1(w) = \frac{\sqrt{-w}}{\pi\Delta_{\parallel}^2} \left[1 + 2 \ln \left(\frac{\psi}{-2w} \right) \right] + \frac{6 + (\sqrt{2} + \sqrt{-w})(1-w)\sqrt{-w}}{\pi(\sqrt{2} + \sqrt{-w})(4-2w+w^2)} \quad \text{for } -2\psi \leq w < 0, \quad (3a)$$

$$F_1(w) = \frac{6\sqrt{2}}{\pi(8+w^3)} \quad \text{for } w > 0. \quad (3b)$$

Equations (3a) and (3b) describe the distributions of the trapped and passing electrons, respectively. The trapped electron distribution has a hollowed out shape, while the passing electron distribution has a flattop shape.

In the simulations, the density is normalized to the unperturbed density n_0 . The velocities are expressed in units of the electron thermal velocity $v_{Te} = (T_e/m_e)^{1/2}$. The dimensionless units used here have space in the Debye length $\lambda_D = (\epsilon_0 T_e / n_0 e^2)^{1/2}$, time in the inverse of the plasma frequency $\omega_{pe} = (n_0 e^2 / m_e \epsilon_0)^{1/2}$, and the potential in T_e/e . The electric field is expressed in unit of $m_e \omega_{pe} v_{Te} / e$ and the magnetic field is expressed in unit of $m_e \omega_{pe} / e$. Grid size units $\lambda_D \times \lambda_D$ are used in the simulations, and the time step is $0.02 \omega_{pe}^{-1}$. There are average 400 particles in each cell, and the number of cells is 128×128 .

In the model, we choose the light speed as $c/v_{Te} = 20.0$. The initial potential of the electron hole is characterized by $\psi = 2.0$ and $\Delta_{\parallel} = 3.0$. Therefore, the bounce frequency of a trapped electron in the electron holes is $\omega_b/\omega_{pe} = 0.47$. The electron gyrofrequency is chosen as $\Omega_e/\omega_{pe} = 0.7$, which is slightly larger than the bounce frequency ω_b . Initially, the electron hole is at rest, and the electrons are loaded according to Eqs. (2) and (3) in our PIC simulations.

III. SIMULATION RESULTS

Figure 1 shows the time evolution of the electric field energies (a) E_x^2 , (b) E_y^2 , and (c) the fluctuating magnetic field energy $\delta B^2 = \delta B_x^2 + \delta B_y^2 + \delta B_z^2$. The electric field energies are normalized by $n_0 T_e / \epsilon_0$ and the magnetic field energy is nor-

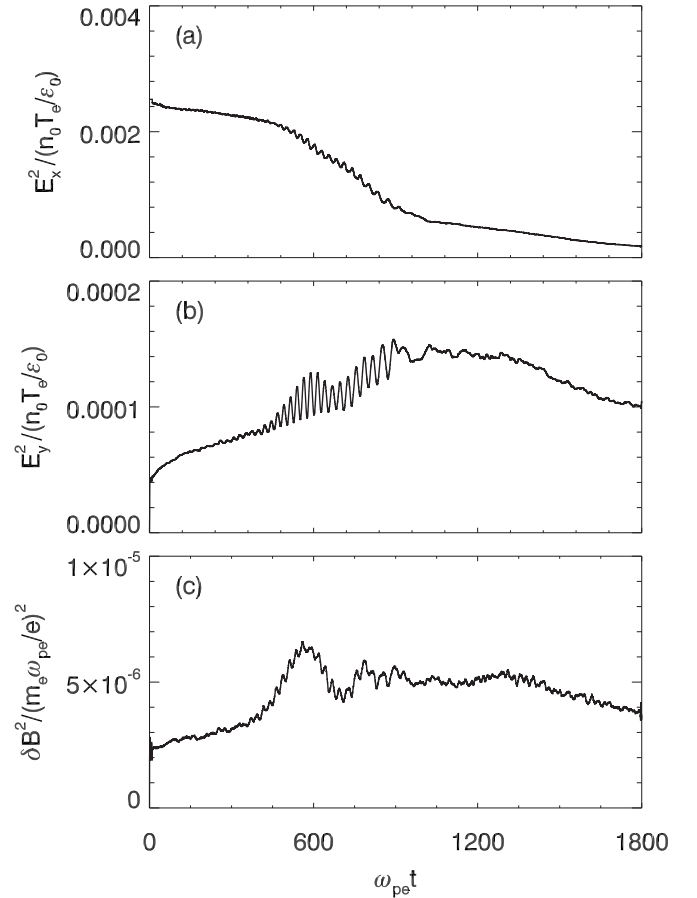


FIG. 1. The time evolution of the electric field energies (a) E_x^2 and (b) E_y^2 and (c) the fluctuating magnetic field energy $\delta B^2 = \delta B_x^2 + \delta B_y^2 + \delta B_z^2$. The electric field energies are normalized by $n_0 T_e / \epsilon_0$ and the magnetic field energy is normalized by $m_e^2 \omega_{pe}^2 / e^2$.

malized by $m_e^2 \omega_{pe}^2 / e^2$. The increase of the electric field energy E_y^2 means the excitation of the transverse instability in the electron hole. As the transverse instability occurs, a kinked electron hole with the existence of the perpendicular electric field E_y is first formed.^{19,20} At the same time, we can find that with the excitation of the transverse instability at about $\omega_{pe} t = 300$, the electric field energy E_x^2 decreases, while the fluctuating magnetic field energy δB^2 and electric field energy E_y^2 increase. The electric field energy E_y^2 attains its maximum value at about $\omega_{pe} t = 920$.

Detailed analysis shows that with the excitation of the transverse instability, the electric field and the fluctuating magnetic field can form regular structures. The evolution of the electric field is shown in Fig. 2, which plots the electric fields (a) E_x and (b) E_y at $\omega_{pe} t = 0, 800$, and 1340 . With the excitation of the transverse instability, a kinked electron hole is first formed, and a series of islands (with alternate positive and negative E_y values) develops in the electron hole due to the combined actions between the transverse instability and the stabilization by the magnetic field. The magnetic field guides the trapped electrons to bounce back and forth along the parallel direction in the electron hole. It can prevent the trapped electrons from being focusing by the transverse gradients of the potential and make the electron hole stable.^{19,20} At last, the electron hole is broken into several 2D electron

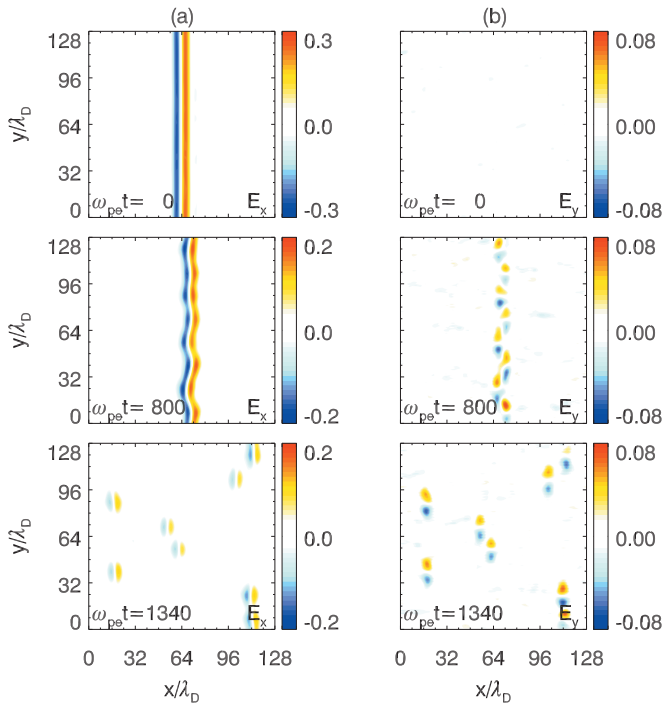


FIG. 2. (Color) The left column shows the electric field component (a) E_x at $\omega_{pe}t=0, 800$, and 1340 . The right column shows the electric field component (b) E_y at $\omega_{pe}t=0, 800$, and 1340 .

holes which are isolated in both the x and y directions. In these 2D electron holes, the parallel cut of E_y has unipolar structures, while the parallel cut of E_x has bipolar structures. At the same time, these electron holes move along the x direction with different speeds, and they can last several thousands of electron plasma periods. This evolution of the electric field is the same as that occurs in 2D electrostatic PIC simulations, which has been described by Wu *et al.*²⁴ Such unipolar structures of E_y , as well as the bipolar structures of E_x , have also been obtained in theoretical studies of multidimensional BGK modes.^{25,26}

However, in the present electromagnetic PIC simulations, the magnetic field in these 2D electron holes is also found to have regular structures. Figure 3 shows the fluctuating magnetic fields (a) δB_x , (b) δB_y , (c) δB_z , (d) v_{Ez} , and (e) j_z at $\omega_{pe}t=1340$. The current is calculated by summing the contributions of all particles in the simulations. In this region, there exist several 2D electron holes. Obviously, at the positions with the existence of 2D electron holes, the parallel cut of the fluctuating magnetic field δB_x has unipolar structures; simultaneously δB_x always has positive value with its maximum value in the center of the electron holes. The fluctuating magnetic field δB_y has quadrupole structures in these electron holes, and the parallel cut of the fluctuating magnetic field δB_y has bipolar structures. For the fluctuating magnetic field δB_z , it is positive in the upper part of these electron holes, while it is negative in the lower part. The parallel cut of δB_z has unipolar structures in these electron holes. Their amplitudes are about $\delta B_x/B_0=0.001$, $\delta B_y/B_0=0.0003$, and $\delta B_z/B_0=0.0006$.

The formation of the magnetic structures associated with the 2D electron holes can be described as follows: these 2D

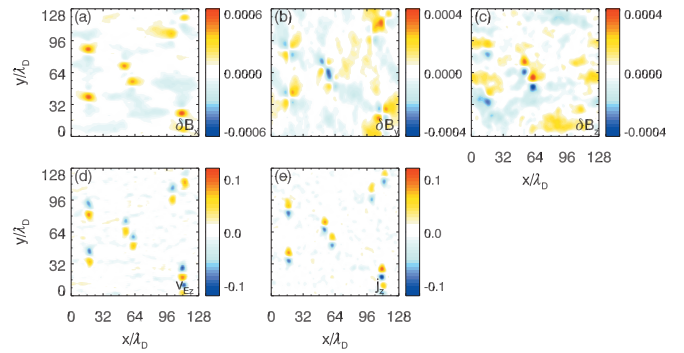


FIG. 3. (Color) The fluctuating magnetic fields (a) δB_x , (b) δB_y , (c) δB_z , (d) v_{Ez} , and (e) j_z at $\omega_{pe}t=1340$.

electron holes can be formed due to the combined action between the transverse instability and the stabilization by the background magnetic field. There exists perpendicular electric field E_y in these electron holes, which is positive in the upper part and negative in the lower part. The trapped electrons in the electron holes will then suffer the electric field drift $\mathbf{v}_E = \mathbf{E} \times \mathbf{B}_0 / B_0^2$, which can be estimated to be about $0.07v_{Te}$ [Fig. 3(d)]. The electric field drift of the trapped electrons in these electron holes then generates the current along the z direction¹⁸ (Ions, which cannot be trapped in the electron holes with positive potential, may also suffer electric field drift in the electron holes. However, their drift motions are too complicated to be described by a simple expression because their gyroradii are larger than the spatial scales of the electron holes and their effects on the current along the z direction are negligible.) From the figure, we can know that the amplitude of j_z is about $0.05n_0e v_{Te}$, which is roughly the same as the value that calculated based on the electric field drift $\mathbf{v}_E = \mathbf{E} \times \mathbf{B}_0 / B_0^2$. The current can then generate the fluctuating magnetic fields δB_x and δB_y in the electron holes, and their parallel cuts have unipolar and bipolar structures, respectively. Based on the Ampere circuital theorem, the amplitudes of the fluctuating magnetic field along the directions parallel and perpendicular to the background magnetic field are estimated to be about $\delta B_x/B_0=0.001$ and $\delta B_y/B_0=0.0005$, which are consistent with the values in Figs. 3(a) and 3(b). At the same time, these 2D electron holes move along the x direction. The structures of the fluctuating magnetic field along the z direction, whose parallel cut has unipolar structures, can be explained by a Lorentz transforming of a moving quasielectrostatic structure.²⁷ The fluctuating magnetic field δB_z can be described as

$$\delta B_z = \frac{v_{EH}}{c^2} E_y, \quad (4)$$

where v_{EH} is the propagation speed of the electron hole, which is parallel to the background magnetic field \mathbf{B}_0 . The propagation speed of the electron holes is about $1.0v_{Te}$, and then $E_y=400v_{Te}\delta B_z$, which is consistent with the simulation results.

IV. DISCUSSION AND CONCLUSION

In summary, we perform 2D PIC simulations to investigate the structures of the fluctuating magnetic field in electron holes. 2D electron holes can be formed due to the combined actions between the transverse instability and the stabilization by the background magnetic field. In these 2D electron holes, the parallel cut of the parallel and perpendicular electric fields has bipolar and unipolar structures, respectively, which have been verified in both satellite observations and simulations.^{13–19} The theoretical theories based on BGK mode have also demonstrated that multidimensional electron holes have similar electrostatic structures.^{25,26} Associated with the 2D electron holes, the parallel cuts of the fluctuating magnetic fields δB_x , δB_y , and δB_z are further found to have unipolar, bipolar, and unipolar structures, respectively.

Recently, Andersson *et al.*²¹ investigated the magnetic structures associated with electron holes in Earth's plasma sheet by THEMIS satellites. These electron holes, whose parallel cuts of the parallel and perpendicular electric fields have bipolar and unipolar structures, respectively, have a significant center potential $\psi \sim T_e/e$. In addition, these electron holes have detectable fluctuating magnetic field with the amplitude $\delta B_{\parallel}/B_0 = 0.001 - 0.005$ and $\delta B_{\perp}/B_0 = 0.0005 - 0.003$ in the directions parallel and perpendicular to the background magnetic field, and their parallel cuts of both δB_{\parallel} and δB_{\perp} (δB_y and δB_z) have unipolar structures. However, our simulations indicate that the perpendicular component of the fluctuating magnetic field δB_y has bipolar structures. The difference may be due to the 3D effects. In a 3D electron hole, there exists the perpendicular electric field E_z . It will then produce the fluctuating magnetic field δB_y with the unipolar structures by a Lorentz transforming if the electron holes propagate along the background magnetic field. If the propagating speed is sufficiently large, we should observe the unipolar structures of δB_y , as found in the observations. However, our simulations imply that bipolar structures for the parallel cut of δB_{\perp} should be observed if the moving speed of the electron holes is sufficiently small, which is to be verified by further satellite observations.

ACKNOWLEDGMENTS

This research was supported by the National Science Foundation of China (NSFC) under Grant Nos. 40725013,

40974081, and 40931053 and the Fundamental Research Funds for the Central Universities (Grant No. WK2080000010).

- ¹H. Matsumoto, H. Kojima, T. Miyatake, Y. Omura, M. Okada, I. Nagano, and M. Tsutsui, *Geophys. Res. Lett.* **21**, 2915, doi:10.1029/94GL01284 (1994).
- ²R. E. Ergun, C. W. Carlson, J. P. McFadden, F. S. Mozer, G. T. Delory, W. Peria, C. C. Chaston, M. Temerin, I. Roth, L. Muschietti, R. Elphic, R. Strangeway, R. Pfaff, C. A. Cattell, D. Klumppar, E. Shelley, W. Peterson, E. Moebius, and L. Kistler, *Geophys. Res. Lett.* **25**, 2041, doi:10.1029/98GL00636 (1998).
- ³S. D. Bale, P. J. Kellogg, D. E. Larsen, R. P. Lin, K. Goetz, and R. P. Lepping, *Geophys. Res. Lett.* **25**, 2929, doi:10.1029/98GL02111 (1998).
- ⁴A. Mangeney, C. Salem, C. Lacombe, J.-L. Bougeret, C. Perche, R. Manning, P. J. Kellogg, K. Goetz, S. J. Monson, and J.-M. Bosqued, *Ann. Geophys.* **17**, 307 (1999).
- ⁵C. Cattell, J. Crumley, J. Dombeck, J. Wygant, and F. S. Mozer, *Geophys. Res. Lett.* **29**, 1065, doi:10.1029/2001GL014046 (2002).
- ⁶J. S. Pickett, L.-J. Chen, S. W. Kahler, O. Santolík, D. A. Gurnett, B. T. Tsurutani, and A. Balogh, *Ann. Geophys.* **22**, 2515 (2004).
- ⁷I. B. Bernstein, J. M. Greene, and M. D. Kruskal, *Phys. Rev.* **108**, 546 (1957).
- ⁸L.-J. Chen, J. Pickett, P. Kintner, J. Franz, and D. Gurnett, *J. Geophys. Res.* **110**, A09211, doi:10.1029/2005JA011087 (2005).
- ⁹C. S. Ng and A. Bhattacharjee, *Phys. Rev. Lett.* **95**, 245004 (2005).
- ¹⁰K. V. Roberts and H. L. Berks, *Phys. Rev. Lett.* **19**, 297 (1967).
- ¹¹Y. Omura, H. Kojima, and H. Matsumoto, *Geophys. Res. Lett.* **21**, 2923, doi:10.1029/94GL01605 (1994).
- ¹²Q. Lu, S. Wang, and X. Dou, *Phys. Plasmas* **12**, 072903 (2005).
- ¹³R. E. Ergun, C. W. Carlson, J. P. McFadden, F. S. Mozer, L. Muschietti, I. Roth, and R. J. Strangeway, *Phys. Rev. Lett.* **81**, 826 (1998).
- ¹⁴J. R. Franz, P. M. Kintner, and J. S. Pickett, *Geophys. Res. Lett.* **25**, 1277, doi:10.1029/98GL50870 (1998).
- ¹⁵J. R. Franz, P. M. Kintner, J. S. Pickett, and L.-J. Chen, *J. Geophys. Res.* **110**, A09212, doi:10.1029/2005JA011095 (2005).
- ¹⁶M. Oppenheim, D. L. Newman, and M. V. Goldman, *Phys. Rev. Lett.* **83**, 2344 (1999).
- ¹⁷M. V. Goldman, M. Oppenheim, and D. L. Newman, *Geophys. Res. Lett.* **26**, 1821, doi:10.1029/1999GL900435 (1999).
- ¹⁸T. Umeda, Y. Omura, and H. Matsumoto, *J. Geophys. Res.* **109**, A02207, doi:10.1029/2003JA010000 (2004).
- ¹⁹Q. M. Lu, B. Lembege, J. B. Tao, and S. Wang, *J. Geophys. Res.* **113**, A11219 (2008).
- ²⁰L. Muschietti, I. Roth, C. W. Carlson, and R. E. Ergun, *Phys. Rev. Lett.* **85**, 94 (2000).
- ²¹L. Andersson, R. E. Ergun, J. Tao, A. Roux, O. LeContel, V. Angelopoulos, J. Bonnell, J. P. McFadden, D. E. Larson, S. Eriksson, T. Johansson, C. M. Cully, D. L. Newman, M. V. Goldman, K.-H. Glassmeier, and W. Baumjohann, *Phys. Rev. Lett.* **102**, 225004 (2009).
- ²²X. R. Fu, Q. M. Lu, and S. Wang, *Phys. Plasmas* **13**, 012309 (2006).
- ²³L. Muschietti, R. E. Ergun, I. Roth, and C. W. Carlson, *Geophys. Res. Lett.* **26**, 1093, doi:10.1029/1999GL900207 (1999).
- ²⁴M. Y. Wu, Q. M. Lu, C. Huang, and S. Wang, *J. Geophys. Res.* **115**, A10245, doi:10.1029/2009JA015235 (2010).
- ²⁵L. J. Chen and G. K. Parks, *Geophys. Res. Lett.* **29**, 1331, doi:10.1029/2001GL013385 (2002).
- ²⁶C. S. Ng and A. Bhattacharjee, *Phys. Plasmas* **13**, 055903 (2006).
- ²⁷J. D. Jackson, *Classical Electrodynamics* (Wiley, New York, 1998), p. 558.